Ground Reaction Force Estimation in Prosthetic Legs with an Extended Kalman Filter

Seyed Abolfazl Fakoorian
Department of Electrical Engineering and Computer Science, Cleveland State University,
Cleveland, Ohio
s.fakoorian@csuohio.edu

Dan Simon
Department of Electrical Engineering and Computer Science, Cleveland State University,
Cleveland, Ohio
d.j.simon@csuohio.edu

Hanz Richter
Department of Mechanical Engineering, Cleveland State University,
Cleveland, Ohio
h.richter@csuohio.edu

Vahid Azimi
Department of Electrical Engineering and Computer Science, Cleveland State University,
Cleveland, Ohio
v.azimi@csuohio.edu

***Abstract*—A method to estimate ground reaction forces (GRFs) in a robot/prosthesis system is presented. The system includes a robot that emulates human hip and thigh motion, along with a powered (active) prosthetic leg for transfemoral amputees, and includes four degrees of freedom (DOF): vertical hip displacement, thigh angle, knee angle, and ankle angle. We design a continuous-time extended Kalman filter (EKF) to estimate not only the states of the robot/prosthesis system, but also the GRFs that act on the prosthetic foot. The simulation results show that the average RMS estimation errors of the thigh, knee, and ankle angles are 0.007, 0.015, and 0.465 rad with the use of four, two, and one measurements respectively. The average GRF estimation errors are 2.914, 7.595, and 20.359 N with the use of four, two, and one measurements respectively. It is shown via simulation that the state estimates remain bounded if the initial estimation errors and the disturbances are sufficiently small.**

Keywords— ground reaction force (GRF); state estimation; prosthetic leg; extended Kalman filter (EKF)

I. INTRODUCTION

Passive lower limb prostheses are not able to contribute any net power to gait, which leads to the expenditure of up 60% more energy by amputees than able-bodied persons [1]. In 1997, Otto Bock introduced the C-leg, which is a semi-active microprocessor-controlled prosthetic knee [2]. Recent advances in microelectronics and robotic technologies have enabled the development of powered prosthetic legs [3] that can help amputees walk up stairs and slopes as easily as able-bodied persons because of the leg's net power contribution to gait; they are also able to adapt their behavior to various environmental conditions. Ossur has recently introduced a lower limb prostheses with powered joints called the Power Knee, which is the first commercially available knee to generate power during the gait cycle [4]. Other powered knee and ankle prostheses have been reported in [5]–[7]. Vanderbilt University has developed a prosthesis with integrated powered knee and ankle joints to increase the mobility of transfemoral amputees [8].

This research was supported by NSF Grant 1344954

In our research, a powered (active) prosthetic leg is considered for transfemoral amputees. The prosthetic leg is coupled with a robotic hip/thigh emulator. The combined system includes four degrees of freedom: vertical hip displacement, thigh angle, knee angle, and ankle angle. Bulky load cells and sensors are often employed in robots and prosthetic legs to capture gait data and external forces (GRFs) and moments during walking [9]. These data are used as feedback measurements to control the robot or prosthesis. The control parameters depend on the gait mode, which is determined on the basis of the external forces. However, there are several drawbacks to the use of load cells: (i) Load cells are expensive; (ii) A 250-lbf load cell weighs about 1 lb, with a length of about 3 inches, and thus does not easily fit in the prosthetic knee; (iii) Load cell measurements tend to drift and need to be frequently offset, and they are also noisy and need good signal conditioning; (iv) Load cells can get damaged easily from overloading or off-axis loading.

The aforementioned problems do not arise with angle sensors because high-resolution encoders are accurate, reliable, and inexpensive. Nevertheless, they do not measure velocity, and velocity calculation from numerical differentiation is usually challenging because of the difficult compromise between noise rejection and bandwidth. There have been several methods to reduce the number of force sensors in robotics. A robot compliance controller based on a disturbance observer is presented in [10], where the disturbance observer is used to estimate the external reaction forces. In [11], a method for force estimation of the end-effector of a SCARA robot is presented. They used the robot dynamic model with servo motor currents and positions to estimate external forces. In [12], the external force on the end-effector of a 4-DOF robot manipulator is estimated. They proposed a new algorithm from the combination of time delay estimation and input estimation.

As far as we know, the present research is the first attempt to estimate GRFs for prostheses without the use of load cells. The Kalman filter (KF), which is the most common method for tracking and estimation because of its optimality, provides us with the opportunity to remove bulky and expensive load cells from the prosthesis, and to reduce the number of sensors.

However, the KF cannot be directly used in nonlinear systems. The EKF, which linearizes the system dynamics using a first-order Taylor series expansion, is frequently applied to estimate the states of nonlinear systems [13]–[16].

The main contribution of this work is the design of an EKF for the online estimation of joint coordinates (hip displacement, thigh angle, knee angle, and ankle angle) and their velocities, the estimation of GRFs, and simulation results from a realistic 4-DOF simulation. First, the dynamic equations of the robotic system, the prosthetic leg, and the GRF are presented. Given the dynamic system equations, we can estimate the system states with four measurements: hip displacement, thigh angle, knee angle, and ankle angle. In the next step, the accuracy of the estimation is explored by using only two measurements: knee and ankle angles. Finally, the accuracy of the estimation is explored using only one measurement: knee angle.

The paper is organized as follows. In Section II the model of the robotic system and prosthetic leg is presented. In Section III the model of the EKF for state estimations and GRF estimation is discussed. Section IV provides simulation results and compares the results when different measurement sensors are used; furthermore, the convergence of the EKF is tested using different initial errors and noise terms. In Section V we conclude the paper and suggest future research.

II. SYSTEM MODEL

The model of the prosthetic leg is based on the standard robotics framework. Fig. 1 shows a diagram of the hip robot and prosthesis combination [17-18]. A general dynamic model for the system is given as follows:

$$D(q)\ddot{q} + C(q,\dot{q})\dot{q} + B(q,\dot{q}) + {J_e}^T F_e + g(q) = u \qquad (1)$$

where $q^T = [q_1 \;\; q_2 \;\; q_3 \;\; q_4]$ is the vector of joint displacements (q_1 is vertical hip displacement, q_2 is thigh angle, q_3 is knee angle, and q_4 is ankle angle), $D(q)$ is the inertia matrix, $C(q,\dot{q})$ is a matrix accounting for centripetal and Coriolis effects, $B(q,\dot{q})$ is a nonlinear damping vector, J_e is the kinematic Jacobian relative to the point of application of the external forces F_e, $g(q)$ is the gravity vector, and u is the four-element vector of control signals [19]. The kinematic and dynamic model of the robot / prosthesis combination are given in [20-23], where a mixed tracking / impedance controller based on passivity methods is designed. The control signals consist of hip force, and thigh, knee, and ankle torques. As Fig. 1 shows, a triangular foot with two points of ground contact is assumed. It can be seen that horizontal and vertical GRFs are applied to the contact points at the toe and heel. The GRFs are denoted as $F_{xh}, F_{zh}, F_{xt}, F_{zt}$, which represent the horizontal and vertical GRFs at the heel and toe. Thus, the external force vector F_e in (1) is comprised of these four GRFs.

We assume the robot walks along the x-axis. A treadmill is used to simulate the walking surface of the robot / prosthesis system. The belt stiffness is modeled to calculate reaction forces during contact between the heel and toe with the belt [19-20]. The GRFs are entirely determined by kinematics and are given as follows [20]:

$$z_h = -0.11\sin(q_2 + q_3 + q_4 - 0.787) + l_3\sin(q_2 + q_3) + l_2\sin(q_2) + q_1 \qquad (2)$$

$$z_t = 0.241\sin(q_2 + q_3 + q_4 + 0.787) + l_3\sin(q_2 + q_3) + l_2\sin(q_2) + q_1 \qquad (3)$$

$$F_{zh} = -k_b\,(z_h - s_z)\left(\frac{1+\mathrm{sign}(z_h - s_z)}{2}\right) \qquad (4)$$

$$F_{zt} = -k_b\,(z_t - s_z)\left(\frac{1+\mathrm{sign}(z_t - s_z)}{2}\right) \qquad (5)$$

$$F_{xh} = \beta F_{zh} \qquad (6)$$

$$F_{xt} = \beta\, F_{zt} \qquad (7)$$

where k_b is the belt stiffness , s_z is the treadmill standoff (the distance between the origin of the world coordinate system and the belt when the leg is fully extended), l_2 and l_3 are the lengths of link 2 (thigh) and link 3 (shank) respectively, and β is the friction coefficient between the belt and the foot. The vertical positions of the toe and heel in the world coordinate system are shown in Fig. 1 as z_t and z_h respectively. We thus have four states for the positions and four states for the velocities of the joint displacements.

One of the main objectives of this research is to estimate the GRFs which comprise F_e in (1). As a result, we need to augment the external forces to the state vector. The augmented state vector comprises the eight original states of the robot and the four GRFs and is given as follows:

$$x = [q_1 \;\; q_2 \;\; q_3 \;\; q_4 \;\; \dot{q}_1 \;\; \dot{q}_2 \;\; \dot{q}_3 \;\; \dot{q}_4 \;\; F_{xt} \;\; F_{zt} \;\; F_{xh} \;\; F_{zh}]^T \qquad (8)$$

Although the forces are static functions of the states, they are treated here as external, independent inputs, and are therefore regarded as states to be estimated. Thus, the 12-element vector of (8) is the vector that is estimated by the state estimator.

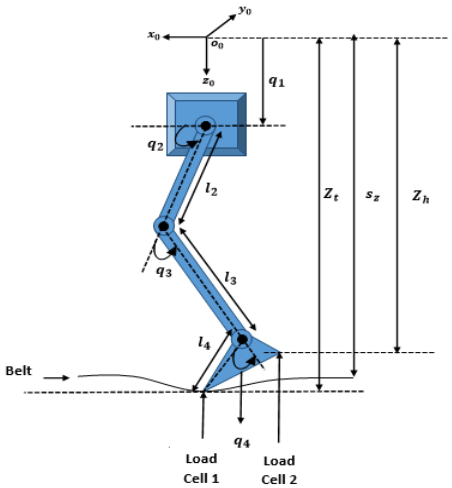

Fig. 1 The robotic model of prosthetic leg

III. EXTENDED KALMAN FILTERING FOR ROBOT / PROSTHISIS STATE ESTIMATION

The Kalman filter applies directly only to linear systems. However, we can linearize a nonlinear system and then use linear estimation techniques. Over the last few decades the extended Kalman filter (EKF) has become one of the most popular estimation techniques in nonlinear systems. The EKF applies the standard linear Kalman filter methodology to a linearization of the nonlinear system [24]. According to the continuous time-EKF equations [25, Part IV], the system and measurement equations are assumed as

$$\dot{x} = f(x,u,t) + G(t)w(t) \quad (9)$$
$$y = h(x,t) + D(t)v(t) \quad (10)$$

where the state $x(t)$, the input $u(t)$, and the output $y(t)$ are in $\mathbb{R}^q$, $\mathbb{R}^p$, and $\mathbb{R}^m$ respectively. Moreover, the noise terms $w(t)$ and $v(t)$ are in $\mathbb{R}^l$ and $\mathbb{R}^k$ and are uncorrelated, zero-mean white noise processes with identity covariance. $G(t)$ and $D(t)$ are time-varying matrices of size $q \times l$ and $m \times k$ for every time $t \geq 0$. If the nonlinear functions f and h are sufficiently smooth in x, Taylor series expansions can be performed. The following Jacobian matrices are used to linearize the system:

$$A = \left.\frac{\partial f}{\partial x}\right|_{\hat{x}} \quad (11)$$

$$C = \left.\frac{\partial h}{\partial x}\right|_{\hat{x}} \quad (12)$$

The initial state estimate $\hat{x}\ (0)$ is a random vector with error covariance $P(0)$:

$$\hat{x}\ (0) = E[x(0)]$$
$$P(0) = E[(x(0) - \hat{x}\ (0))(x(0) - \hat{x}\ (0))^T]$$

and $\hat{x}\ (0)$ is assumed to be uncorrelated with w and v. The EKF equations are given as

$$\dot{\hat{x}} = f(\hat{x},u,t) + K[y - h(\hat{x},t)] \quad (13)$$
$$K(t) = P(t)C^T(t)R^{-1}(t) \quad (14)$$
$$\dot{P}(t) = A(t)P(t) + P(t)A^T(t) + Q(t) - P(t)C^T(t)R^{-1}(t)C(t)P(t) \quad (15)$$

where $K(t)$ and $P(t)$ are the Kalman gain and estimation error covariance matrix. Covariance matrices $Q(t)$ and $R(t)$ are $q \times q$ and $m \times m$ respectively, and are defined as follows:

$$Q(t) = G(t)G^T(t) \quad (16)$$
$$R(t) = D(t)D^T(t) \quad (17)$$

The state space equations of the robotic / prosthetic system can be obtained from (1) and the GRF equations must be differentiated to obtain the state space model of the GRF. However, the nonlinearity of these equations can be problematic.

There are two ways to handle this problem. First, we can use a smooth approximation of the sign function using the *tanh* function; but this approach requires a lot of computational effort for the Jacobian calculation and typically results in EKF divergence [26]. In the second approach, which is used in this paper, the sign function is not considered when we take the derivative of (2)–(7) to include the GRFs in the state space model. The sign function is re-introduced in the computed Jacobian matrix after taking the derivative. The state space equations of the GRFs are given as follows:

$$\dot{F_{zh}} = -k_b\, \dot{z_h} \left(\frac{1+\text{sign}(z_h - s_z)}{2}\right) \quad (18)$$
$$\dot{F_{zt}} = -k_b\, \dot{z_t} \left(\frac{1+\text{sign}(z_h - s_t)}{2}\right) \quad (19)$$
$$\dot{F_{xh}} = \beta\, \dot{F_{zh}} \quad (20)$$
$$\dot{F_{xt}} = \beta\, \dot{F_{zt}} \quad (21)$$

where $\dot{z_h}$, $\dot{z_t}$ represent the derivatives of (2) and (3).

IV. SIMULATION RESULTS

The performance of the prosthetic leg during one step of normal walking which lasts approximately one second, is considered here. The reference data here are provided by able-bodied research participants at the motion studies laboratory (MSL) of the Cleveland Department of Veterans Affairs Medical Center (VAMC) [27]. In the robot / prosthesis system, we have 12 states estimates, so the A matrix in (11) is 12×12. We use 4 states as the measurements: vertical hip position, thigh angle, knee angle and ankle angle. Thus, the dimension of the measurement matrix C in (12) is 4×12. The initial value of the system's state vector $x(0)$ is obtained from the reference data, and we randomly choose the initial condition of the estimated state vector $\hat{x}(0)$ to be close to the initial reference data but with some reasonable error.

$$x(0) = [0.019 \quad 1.13 \quad 0.09 \quad -2.246 \quad 0.093 \quad 0.77 \quad 1.41 \quad 2.89 \quad 0 \quad 0 \quad 0 \quad 0]^T$$
$$\hat{x}(0) = [0.04 \quad 0.901 \quad 0.292 \quad -2.44 \quad 0.293 \quad 0.43 \quad 1.112 \quad 2.62 \quad 0 \quad 0 \quad 0 \quad 0]^T$$

We will analytically consider the region of attraction for the state estimator in future work; however, in this paper, we examine the convergence of the EKF via simulation.

The diagonal covariance matrices of the continuous-time process noise Q and measurement noise R are considered as follows:

$$Q = Q_d/\Delta t = \text{diag}[0.0005 \quad 0.0005 \quad 0.0005 \quad 0.0005 \quad 0.0002 \quad 0.0002 \quad 0.0002 \quad 0.0002 \quad 0 \quad 0 \quad 0 \quad 0]/\Delta t$$

$$R = R_d \Delta t = \text{diag}[10^{-3}\ 10^{-3}\ 10^{-3}\ 10^{-3}]\Delta t$$

where $\Delta t = 0.5$ ms denotes the discretization step size , and the relationships between the continuous-time and discrete-time noise covariances are given in [25, Chap.8].

The process noise Q partially accounts for unmodeled dynamics and parameter uncertainties. The R matrix is usually straightforward to determine on the basis of our knowledge of the accuracy of the measurement equipment. Our simulations are developed in continuous time (and discretized by Matlab Simulink) with a fixed integration step size, so we use the discretized covariance matrices Q_d and R_d to incorporate process and measurement noise into the system at each time step.

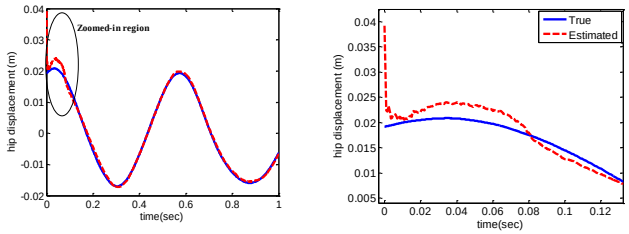

Fig. 2 The left figure shows estimate of the hip displacement. The right plot shows the zoomed-in region.

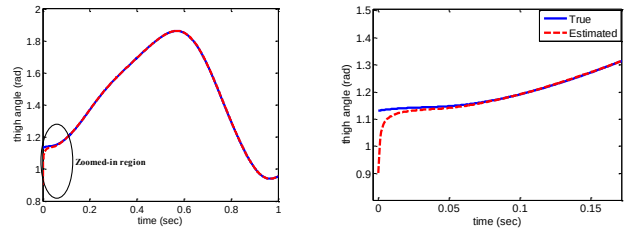

Fig. 3 The left figure shows estimate of the thigh angle. The right plot shows the zoomed-in region.

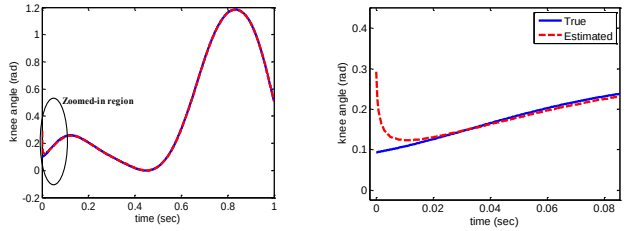

Fig. 4 The left figure shows estimate of the knee angle. The right plot shows the zoomed-in region.

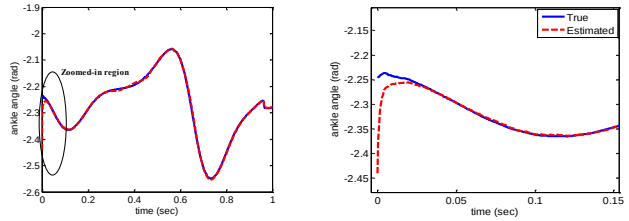

Fig. 5 The left figure shows estimate of the ankle angle. The right plot shows the zoomed-in region.

The state estimation results are shown in Figs. 2–6, which show position and velocity estimates, and Fig. 7, which shows GRF estimates. The zoomed-in regions show that the EKF can estimate the reference states well, even with non-zero initial errors. Although significant initial estimation errors are considered for joint displacements and velocities, the EKF converges to the true states quickly, and estimation performance is satisfactory (Figs. 2–6).

When ankle angle (q_4) changes, the foot rotates around the ankle, which makes the angular velocity of ankle relatively noisy (Fig. 6d).The simulation of the foot rotation starts at heel strike and ends at toe-off (Fig.7; at toe-off the toe lifts off the ground at the end of stance phase). After toe-off there is no foot contact and the GRF is zero.

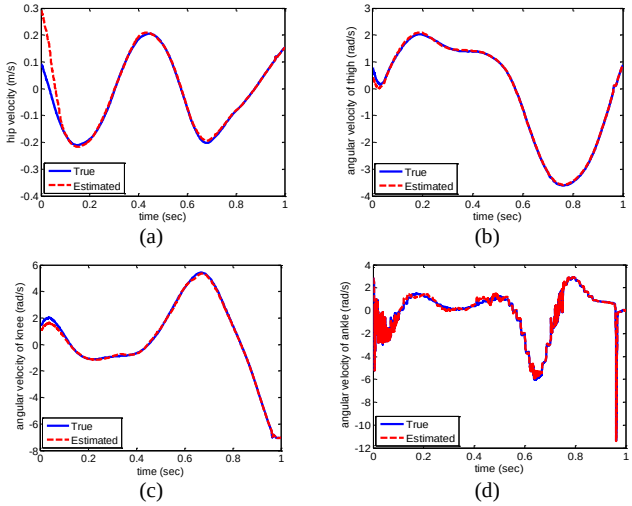

Fig.6 State estimation of the robot velocities

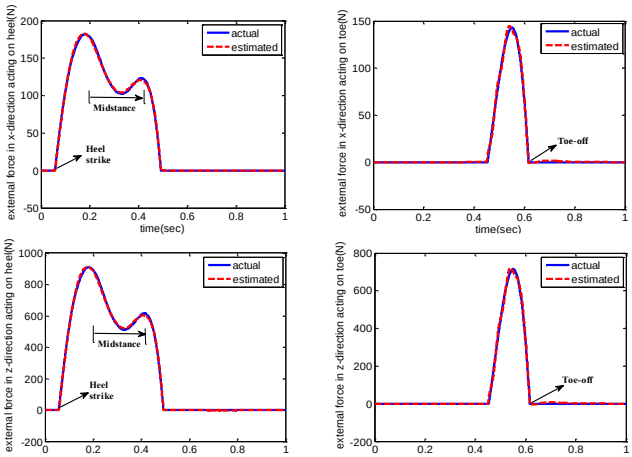

Fig. 7 Horizontal and vertical ground forces (GRFs) estimations

Reduced Measurement Set

More observations result in more accurate state estimation. However, our goal is to use the fewest possible number of sensors for estimation, so we want to reduce the number of measurements. In this case, we use the knee and ankle angles as observations. For our final test, we use only the knee angle as our observation. We define normalized cost functions as follows

$$C_j = \sum_{i=1}^{n} \frac{RMSE_{ij}}{\max\limits_{t\in[0,T]} RMSE_{ij}} \quad i = 1,2,\dots,n \text{ and } j = 1,2,4 \qquad (22)$$

Table I: RMSE for state estimations of the prosthetic leg with different number of measurements and non-zero initial estimation errors

	x_1 (m)	x_2 (rad)	x_3 (rad)	x_4 (rad)	x_5 (m/s)	x_6 (rad/s)	x_7 (rad/s)	x_8 (rad/s)	x_9 (N)	x_{10} (N)	x_{11} (N)	x_{12} (N)	Cost Eq. (22)
Four measurements	0.0004	0.009	0.007	0.005	0.031	0.049	0.091	0.152	1.002	3.966	1.012	5.678	1.368
Two measurements	0.052	0.038	0.032	0.045	0.242	0.823	0.186	0.954	5.124	10.124	3.512	11.621	2.298
One measurement	0.075	0.521	0.781	0.095	2.112	2.414	1.814	2.154	13.05	25.481	14.451	28.452	6.737

where $RMSE_{ij}$ is the root mean square estimation error of the i^{th} state when using j measurements, n is the number of states (12 in our case), and T is the simulation length. Table I compares the accuracy of the state estimation in terms of RMSE and normalized cost. It can be seen, as expected, that the estimation errors with four measurements are smaller than when the estimates are derived using two or one measurements.

Convergence

We next test the convergence of the proposed EKF for the robot / prosthesis system. For this purpose, the initial value $\hat{x}(0)$ as well as the measurement and process noise covariance matrices R, and Q are chosen as shown in Table II. The simulation results are presented in Figs. 8–10, where the unknown state $x_6(t)$ in (8) (angular velocity of thigh), the estimated state $\hat{x}_6(t)$, and its estimation error $\xi_6(t)$ are plotted.

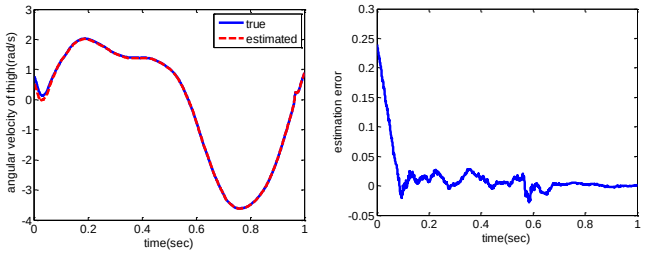

(a) (b)

Fig. 8 The simulation results show the boundedness of the estimation error with small initial error and small noise terms. The sixth state is used here for illustration purposes, but similar results hold for all of the other states as well. (a) is the estimate of $x_6(t)$, and (b) is the estimation error $\xi_6(t)$

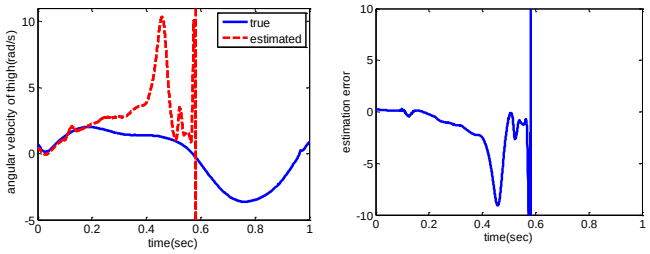

(a) (b)

Fig.9 The simulation results show the divergence of the estimation error with small initial error and large noise terms. The sixth state is used here for illustration purposes, but similar results hold for all of the other states as well. (a) is the estimate of $x_6(t)$ and (b) is the estimation error $\xi_6(t)$

We can see in Fig. 8 that for small initial estimation error and small noise, the estimation error is bounded. However, Figs. 9-10 show that for large initial estimation errors or large noise magnitudes, the estimation error is no longer bounded.

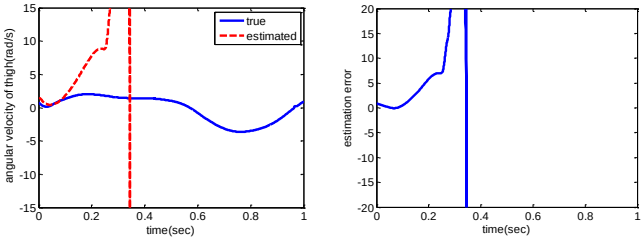

(a) (b)

Fig.10 The simulation results show the divergence of the estimation error with large initial error and small noise terms. The sixth state is used here for illustration purposes, but similar results hold for all of the other states as well. (a) is the estimate of $x_6(t)$ and (b) is the estimation error $\xi_6(t)$

$$\hat{x}_{good}(0) = [0.027 \quad 1.091 \quad 0.112 \quad -2.35 \quad 0.193 \quad 0.539 \quad 1.312 \quad 2.797 \quad 0 \quad 0 \quad 0 \quad 0]^T$$

$$\hat{x}_{poor}(0) = [0.181 \quad 1.991 \quad 0.712 \quad -2.714 \quad 0.393 \quad 1.691 \quad 2.112 \quad 3.44 \quad 0 \quad 0 \quad 0 \quad 0]^T$$

Table II: Initial values and covariance matrices noise terms

	Small initial error and small noise	Small initial error and large noise	Large initial error and small noise
$\hat{x}(0)$	$\hat{x}_{good}(0)$	$\hat{x}_{good}(0)$	$\hat{x}_{poor}(0)$
Q_d	$10^{-5}I_{12\times12}$	$10^{-2}I_{12\times12}$	$10^{-5}I_{12\times12}$
R_d	$10^{-4}I_{4\times4}$	$I_{4\times4}$	$10^{-4}I_{4\times4}$
Error behavior	Bounded	Divergent	Divergent
Figures	Fig. 8	Fig. 9	Fig. 10

V. CONCLUSION AND FUTURE WORK

We designed an EKF to estimate not only the states of a robot / prosthesis system, but also the external forces acting on the prosthetic foot. This technology eliminates the need for heavy and bulky load cells that are otherwise needed for GRF estimation. The average of the thigh, knee, and ankle RMS estimation errors using one, two, and four measurements are 0.465, 0.015, and 0.007 rad respectively; and the average GRF estimation errors are 20.359, 7.595, and 2.914 N respectively. In simulation tests we also showed that the estimation errors remained bounded for small initial estimation errors and small disturbances. However, the filter performance breaks down if the initial estimation errors or disturbances are too large.

In future work we will analytically prove the stability of the continuous-time EKF given certain quantitative conditions on the initial estimation error and disturbance magnitudes. We will also investigate the effects on the convergence of EKF of ignoring the static coupling between the forces and the states. Future work will also focus on improving the estimation results presented here. The EKF has two important potential drawbacks. First, the derivation of the Jacobian matrix for the linearization of the system can be complex and can cause numerical implementation difficulties. Second, linearization can lead to cumulative errors which may affect the accuracy of the state estimation and consequently the stability of the estimation-based control loop. To overcome these limitations, other nonlinear estimators will be explored, such as the unscented Kalman filter (UKF), the H-infinity filter, the particle filter, or the derivative-free Kalman filter (DKF). Unlike the EKF, these filters provide state estimation of nonlinear systems without Jacobian calculations. However, these alternative estimators may require more computational effort than the EKF, which will be a consideration for real-time implementation. Future work will include not only the development of alternative nonlinear estimators such as the UKF, particle filter, and DKF, but will also provide mathematical analyses to ensure that they provide robustness in the presence of system parameter uncertainties, disturbances, and initial estimation errors.

REFERENCES

[1] S.K Au and H. Herr, "Powered ankle-foot prosthesis," *IEEE Robotics and Automation Magazine*, vol. 15 (3), pp. 52–59, Sep. 2008.

[2] A. Segal et al, "Kinematic and kinetic comparisons of transfemoral amputee gait using C-Leg and Mauch SNS prosthetic knees," *Journal of Rehabilitation Research and Development*, vol. 43 (7), pp. 857–870, 2006.

[3] F. Sub and H.A. Varol, "Upslope walking with a Powered Knee and Ankle Prosthesis: Initial results with an amputee Subject," *IEEE Trans. Neural Systems and Rehabilitation Engineering*, vol. 19 (1), pp. 71–78, Oct. 2010.

[4] Z. Harvey, Z. Benjamin, J. Vandersea and E. Wolf, "Prosthetic advances," *Journal of Surgical Orthopedic Advances*, vol. 21 (1), pp. 58–64, Nov. 2011.

[5] C. Martinez, J. Weber, G. Elliott and H. Herr "Design of an agonist-Antagonist active knee prosthesis," in *Proc. IEEE/RAS-EMBS Int. Conf. Biomedical and Robotic*, Scottsdale, AZ, pp. 529–534, 2008.

[6] S.K. Au and H. Herr, "Powered ankle-foot prosthesis for the improvement of amputee ambulation," in *Proc. 29th Annual IEEE Conf. Engineering in Medicine and Biology Society*, Lyon, France, pp. 3020–3026, Aug. 2007.

[7] S.K. Au and J. Weber, "Biomechanical design of a powered ankle-foot prosthesis**,**" in *Proc. IEEE Int. Conf. Rehabilitation Robotics*, Noordwijk, The Netherlands, pp. 298–303, June 2007.

[8] F. Sup, H. Varol, J Mitchell, T. Withrow, "Preliminary evaluations of a self-Contained anthropomorphic transfemoral prosthesis," *IEEE Trans. Mechatronics*, vol. 14 (6), pp. 667–676, Dec. 2009.

[9] M.D. Gonzalez, "Biomechanical analysis of gait kinetics resulting from use of a vacuum socket on a transtibial prosthesis," M.S. thesis, Dept. Mechanical Eng., Univ. of Nevada, Las Vegas, 2014.

[10] T. Murakami, R. Nakamura, F. Yu and K. Ohnishi "Force sensorless impedance control by disturbance observer," *IEEE Conf. Record of the Power Conversion Conference*, Yokohama, Japan, pp. 352–357, April 1993.

[11] J. Simpson, C. Cook and Z. Li, "Sensorless force estimation for robots with friction," *Australasian Conference on Robotics and Automation*, Auckland, pp. 94–99, Nov. 2002.

[12] L. Phong, J. Choi, W. Lee and S. Kang, "A novel method for estimating external force: simulation study with a 4-DOF robot manipulator," *Int. Journal of precision engineering and manufacturing*, vol. 16 (4), pp. 755–766, 2015.

[13] G. G. Rigatos, "A derivative-free Kalman filtering to state estimation-based control of a class of nonlinear system," *IEEE Trans. Ind. Electron.*, vol. 59 (10), pp. 3987–3997, Oct. 2012.

[14] J. Xiong, An Introduction to Stochastic Filtering Theory. London, U.K.: Oxford Univ. Press, 2008.

[15] A. Bryson and Y. Ho, *Applied Optimal Control*. Wiley New York, 1975.

[16] R. Izanloo, S. A. Fakoorian, H. Sadoghi and D. Simon, "Kalman filtering based on the maximum correntropy criterion in the presence of non-Gaussian noise," *50th Annual Conference on Information Science and Systems*, Princeton, New Jersey, March 2016.

[17] H. Richter, D. Simon, W. Smith and S. Samorezov, "Dynamic modeling, parameter estimation and control of a leg prosthesis test robot," *Applied Mathematical Modelling*, vol. 39 (12), pp. 559– 573, 2015.

[18] V. Azimi, D. Simon and H. Richter, "Stable Robust Adaptive Impedance Control of a Prosthetic Leg," *Proceedings of the ASME Dynamic Systems and Control Conference*, Columbus, Ohio, 2015.

[19] H. Mohammadi and H. Richter, "Robust Tracking/Impedance Control: Application to Prosthetics," *American Control Conference*, Chicago, Illinois, pp. 2673–2678, July 2015.

[20] H. Warner, "Optimal design and control of a lower-limb prosthesis with energy regeneration," M.S. thesis, Dept. Mechanical Eng., Cleveland State Univ., Ohio, Aug. 2015.

[21] V. Azimi, D. Simon, H. Richter and S. A. Fakoorian, "Robust composite adaptive transfemoral prosthesis control with non-scalar boundary layer trajectories," *American Control Conference*, Boston, Massachusetts, July 2016.

[22] E. Donald, D. Simon and H. Richter, "Hybrid function approximation based control with application to prosthetic legs," *IEEE Int. Systems Conference*, Orlando, Florida, April 2016.

[23] H. Warner, D. Simon, H. Mohammadi, and H. Richter, "Switched robust tracking/impedance control for an active transfemoral Prosthesis," *American Control Conference*, Boston, Massachusetts, July 2016.

[24] R. Van der Merwe and E.A. Wan "The square-root unscented Kalman filter for state and parameter-estimation," IEEE Int. Conference on ICASSP, Salt Lake City, UT, pp. 3461-3464, 2001.

[25] D. Simon, *Optimal State Estimation: Kalman, H Infinity, and Nonlinear Approaches*, John Wiley & Sons, 2006.

[26] S. Julier, K. Uhlmann and H. Durrant, "A new approach for filtering nonlinear systems," *American Control Conference*, Seattle, Washington, pp. 1628-1632, June 1995

[27] G. Khademi, H. Mohammadi, E. C. Hardin and D. Simon, "Evoluionary optimization of user intent recognition for transfemoral Amputees," Biomedical Circuits and Systems Conference, Atlanta, Georgia, Oct. 2015.